Journal of Orthopaedic Translation 34 (2022) 11–21

Contents lists available at ScienceDirect

Journal of Orthopaedic Translation

journal homepage: www.journals.elsevier.com/journal-of-orthopaedic-translation

# MFG-E8 promotes tendon-bone healing by regualting macrophage efferocytosis and M2 polarization after anterior cruciate ligament reconstruction

Rui Geng [a,b], Yucheng Lin [a,b], Mingliang Ji [a,b], Qing Chang [a,b], Zhuang Li [a,b], Li Xu [a,b], Weituo Zhang [a,b], Jun Lu [a,b,*]

[a] School of Medicine, Southeast University, No. 87 Dingjiaqiao road, 210009, Nanjing, Jiangsu Province, China
[b] Sports Medicine Center, Department of Orthopaedic Surgery, Zhongda Hospital Affiliated to Southeast University, No. 87 Dingjiaqiao road, 210009, Nanjing, Jiangsu Province, China

ARTICLE INFO

*Keywords:*
Anterior cruciate ligament reconstruction
Tendon-bone healing
Milk fat globulin protein E8
Efferocytosis
Macrophage polarization

ABSTRACT

*Background:* Scar tissue formation at the tendon-bone interface caused by excessive inflammation leads to insufficient healing strength, while the phagocytic clearance of dying cells (efferocytosis) has profound consequences on macrophage polarisation and the inflammatory response. Modulating the inflammatory microenvironment may have satisfactory curative effects in patients with anterior cruciate ligament reconstruction (ACLR).
*Methods:* Bone marrow-derived macrophages (BMDMs) and polymorphonuclear leukocytes (PMNs) were harvested from bone marrow. The effects of milk fat globulin protein E8 (MFG-E8) on macrophage polarisation were compared with those of M1 and M2 macrophages induced by conventional methods. The BMDMs and apoptotic PMNs co-culture system was used to assess the efficiency of efferocytosis. The biological functions of MFG-E8 in tendon-bone healing by regulating macrophage efferocytosis and polarisation were further investigated using a rat ACLR model.
*Results:* BMDMs and PMNs were successfully isolated. Compared to conventional induction methods, MFG-E8 alone did not significantly induce macrophage M1 or M2 polarisation, but it could partially reverse the expression of inducible nitric oxide synthase (iNOS) in M1 macrophages. In vitro studies revealed that appropriate dosing of MFG-E8 could significantly promote the efficiency of macrophage efferocytosis and subsequently increase M2 polarisation. More importantly, significantly increased peri-tunnel new bone formation, tighter connected interface and better mechanical properties were observed after ACLR when treated with MFG-E8 in vivo. We further demonstrated that MFG-E8 remarkably facilitated the clearance of apoptotic cells and increased the number of M2 macrophages at the interface between the tendon graft and bone tunnel in the early postoperative stage.
*Conclusion:* MFG-E8 promoted tendon-bone healing histologically and biomechanically, probably by the regulation of inflammatory processes via macrophage efferocytosis and M2 polarisation.
**The translational potential of this article**: Regulation of macrophage efferocytosis and M2 polarization by MFG-E8 is expected to be a therapeutic strategy for promoting tendon-bone healing in patients undergoing ACLR.

## 1. Introduction

Tendon autografts are most commonly used in anterior cruciate ligament (ACL) reconstruction [1]. In the early stage of healing, inflammatory cells are recruited into the tendon-bone interface. The acute inflammation then gradually subsides following the stage of cell proliferation and angiogenesis, ultimately resulting in granulation formation and scar tissue maturation [2]. However, the scar tissue connecting the bone tunnel and tendon graft lacks the biomechanical properties of the native ACL enthesis, which may lead to a lower quality of integration and remodelling between the graft and bone tunnel [3]. Inflammation has been implicated as a critical driver of excessive scar tissue formation or fibrosis in various tissues [4]. Reduction of excessive inflammation and scar formation may result in satisfactory clinical outcomes [5].

* Corresponding author. School of Medicine, Southeast University, No. 87 Dingjiaqiao road, 210009, Nanjing, Jiangsu Province, China.
*E-mail address:* junlusuper@163.com (J. Lu).

https://doi.org/10.1016/j.jot.2022.04.002
Received 12 January 2022; Received in revised form 18 March 2022; Accepted 15 April 2022

Polymorphonuclear leukocytes (PMNs) are an essential component of inflammatory cells that are typically recruited to the tendon-bone interface within seconds and chemoattract monocytes/macrophages to aggregate and proliferate during the early stage after surgery [6]. Subsequently, most PMNs undergo rapid apoptosis and begin to accumulate as uncleared apoptotic cells. However, apoptotic cells contain a large number of autoantigens and cytotoxic compounds, thereby exacerbating the inflammatory response and causing excessive scar formation [7]. Efferocytosis refers to the process of phagocytosis and removal of apoptotic cells by macrophages before they undergo further necrosis and release of high levels of pro-inflammatory cytokines [8]; thus, efferocytosis plays a critical role in resolving inflammation.

Milk fat globulin protein E8 (MFG-E8) is widely expressed in various mammalian cell and tissue types and can bridge macrophages and apoptotic cells during efferocytosis [9]. This process can stimulate macrophages to develop into the anti-inflammatory M2 phenotype [10]. Furthermore, MFG-E8 has been linked to tissue repair in several disease models, such as rescue inflammatory bone loss [11], promotion of angiogenesis in cutaneous wounds [12], and healing of tendon rupture [13].

Therefore, we hypothesised that early application of MFG-E8 after surgery could enhance efferocytosis and M2 polarisation of macrophages, thereby reducing the inflammatory response and eventually promoting tendon-bone healing. We established an ACL reconstruction (ACLR) model to test this hypothesis.

## 2. Methods

### 2.1. Steps of experiments

This study consists of three parts. First, we isolated and characterised bone marrow-derived macrophages (BMDMs) and PMNs. Next, we investigated the effects of MFG-E8 on macrophage efferocytosis and polarisation in vitro. Third, we immersed MFG-E8 into an injectable hydrogel that is commercially available and evaluated the effects of MFG-E8 on tendon-bone healing in vivo. Six-week-old male C57BL/6 mice were used for in vitro studies. Twelve-week-old male Sprague–Dawley (SD) rats were used to establish the ACLR model and for the in vivo evaluation (Fig. 1). The experimental protocols and procedures were approved by the Institutional Animal Care and Use Committee of Southeast University and complied with the ARRIVE guidelines.

### 2.2. BMDM isolation and identification

BMDMs can be obtained by the differentiation of bone marrow cells, as described previously [14]. The humerus, femur, and tibia were harvested from 6-week-old male C57BL/6 mice and were sterilised by soaking in 75% alcohol for 10 s. The bone cavity was flushed with cold phosphate-buffered saline (PBS), and the cell suspension was filtered through a 70 μm cell strainer to obtain a single-cell suspension. The harvested cells were seeded in a medium containing 15% foetal bovine serum and 20 ng/mL recombinant macrophage colony-stimulating factor (M-CSF) (Peprotech, Rocky Hill, NJ, USA). After 3 days, half of the medium was replaced with fresh medium, and BMDMs were strongly attached to the plate after 6 days. Flow cytometry (FCM) was performed by the standard methods to identify BMDMs using primary antibodies against F4/80, CD11b, and their isotype controls (Invitrogen, Carlsbad, CA, USA). The expression of F4/80 and CD11b (Abcam, Cambridge, UK) was validated by double immunofluorescence (IF) staining.

### 2.3. BMDM stimulations

BMDMs were cultured in a 6-well plate. The control group was not treated. To induce M1 or M2 polarisation, 20 ng/mL interferon γ (IFN-γ) (Peprotech, Rocky Hill, NJ, USA) and 100 ng/mL lipopolysaccharide (LPS) (Sigma–Aldrich, St Louis, MO, USA) or 20 ng/mL interleukin 4 (IL-4) (Peprotech, Rocky Hill, NJ, USA) were dissolved in complete medium. To determine the effects of MFG-E8 on macrophage polarisation, 20 ng/mL MFG-E8 (R&D Systems, Minneapolis, MN, USA) was added to complete medium. FCM was performed to identify the phenotype of BMDMs using primary antibodies against CD86 and CD206 (Invitrogen, Carlsbad, CA, USA). IF staining was performed to assess iNOS and CD206 expression (Abcam, Cambridge, UK).

### 2.4. Reverse transcription and quantitative polymerase chain reaction (RT-qPCR)

Total RNA was extracted from cultured cells using TRIzol reagent (Invitrogen, Carlsbad, CA, USA). cDNA was generated using a HiScrip® II 1st Strand cDNA Synthesis Kit (Vazyme, Nanjing, China), according to the manufacturer's protocol. RT-qPCR was conducted in triplicate using a 7900 real-time system (Applied Biosystems, Foster City, CA, USA) with SYBR Green Master Mix (Vazyme, Nanjing, China). The primer sequences are listed in Supplementary File Table S1. Glyceraldehyde-3-phosphate

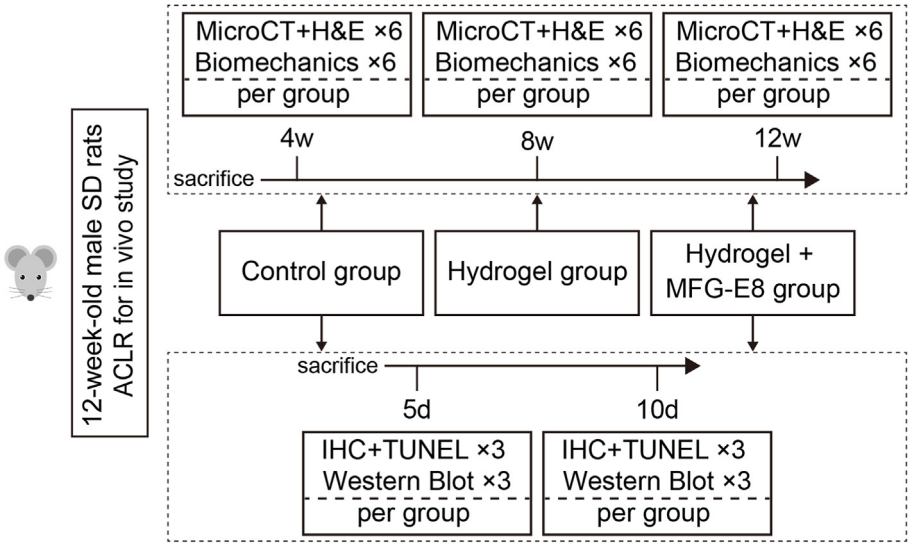


**Figure 1.** Flow chart of the group allocation and analysis items at specific time points for in vivo study. SD, Sprague–Dawley; ACLR, anterior cruciate ligament reconstruction; MFG-E8, milk fat globulin protein E8; H&E, hematoxylin and eosin; IHC, immunohistochemical.

dehydrogenase (GAPDH) was used as a housekeeping gene. The outcomes were analysed using the $2^{-\Delta\Delta Ct}$ method.

### 2.5. PMN isolation and identification

PMNs were prepared as previously described [15]. Briefly, bone marrow cells were aseptically obtained from the humerus, femur, and tibia of 6-week-old male C57BL/6 mice. Percoll™ (GE Healthcare, Pittsburgh, PA, USA) density gradients (81%, 62% and 55%) were used to isolate the PMNs. After gradient centrifugation, PMNs were collected between 81% and 62% layers, and cell morphology was assessed microscopically by modified Giemsa staining. FCM was performed to identify the PMN phenotype using the primary antibodies F4/80, Ly6G, and CD11b (Invitrogen, Carlsbad, CA, USA).

### 2.6. Apoptotic PMN induction

Following isolation and identification, PMNs were starved in serum-free medium for 12, 24, 36, and 48 h to induce apoptosis. The apoptotic rates were then quantified by FCM using Annexin V-FITC and PI (KeyGen BioTech, Nanjing, China).

### 2.7. Efferocytosis assay

Efferocytosis assay was performed as described previously [16]. Briefly, BMDMs were seeded in a 6-well plate for adherent growth and were subsequently stained with DiI and Hoechst 33342 (Beyotime, Shanghai, China) for 5 min. After that, ten-fold TUNEL (Beyotime, Shanghai, China) -labelled apoptotic PMNs (serum-starved for 48 h) were added to the wells. Additionally, different doses of MFG-E8 were administered to the experimental groups. After being co-cultured for 2 h, the plates were washed three times with PBS to remove unengulfed and suspended PMNs. The ability of BMDMs to engulf apoptotic cells was visualised from images captured using a fluorescence microscope (Olympus, Tokyo, Japan). The relative efferocytosis index was calculated by manually counting $>$ 100 cells per field using the following formula [*number of BMDMs containing apoptotic PMNs/total number of BMDMs*] $\times$ 100%. At least three different fields per sample and three samples were analysed.

### 2.8. Preparation and characterisation of the MFG-E8 and hydrogel mixture

Considering that direct application of the MFG-E8 solution may result in its loss from the bone tunnel within a short time, biodegradable ultraviolet (UV) -sensitive hydrogel GelMA 30 (EFL, Suzhou, China) was used as a sustained delivery system. The phase of the hydrogel exhibited a transition from flow liquid sol to viscous glue-like after irradiation with 405 nm UV light for 10 s. First, 5% GelMA solution was prepared according to the manufacturer's instructions. Then, 500 ng of MFG-E8 was immersed in 1 mL GelMA solution and mixed slowly for 10 min. The tested mixture sample was immersed in 50 mL of PBS. The in vitro release test was performed using a 708-DS dissolution system (Agilent, Santa Clara, CA, USA) under the constant conditions of 50 rpm and 37 °C. After the time intervals, 1 mL of the release medium was collected for assaying, and the release medium was subsequently compensated with an equivalent volume of fresh PBS. The cumulative release rate was measured using a UV-spectrophotometer at 429 nm, following the manufacturer's instructions. All release tests were performed in sextuplicate.

The in vitro degradation behaviour of the mixture was investigated by incubation in a complete medium. Briefly, 1 mL of the mixture was dropped on a clean slide and irradiated with 405 nm UV light for 10 s. After that, the mixture was cultured in complete medium in a 37 °C incubator. At specific time points, the mixture and slide were weighed together and recorded after removing the excess water with absorbent paper. The degradation rate was calculated based on the weight loss of the mixture.

### 2.9. Establishment of the ACLR model

Twelve-week-old male SD rats were used to establish the ACLR model as previously described [17,18]. Animals were randomly divided into three groups: control, hygrogel, and hydrogel + MFG-E8. The flexor digitorum longus (FDL) tendon graft (average length, 25 mm) was harvested from the ipsilateral limb through small incisions in the ankle and plantar foot. Both tendon ends were reinforced with a ‘‘whip suture’’ using 5-0 Surgipro™ II (Covidien, St. Louis, MO, USA). A second incision was made anterior to the knee joint and the native ACL was transacted. The drawer test was performed to confirm the integrity of the posterior cruciate ligament. Bone tunnels in the proximal tibia and distal femur were created through the footprint of the native ACL using an electronic drill with a 1.2 mm-diameter Kirschner wire. After soaking the tendon graft in the prepared saline, hydrogel, or hydrogel containing MFG-E8 (500 ng/mL) for 30 s, they were irradiated with 405 nm UV light for 10 s. Furthermore, an additional 0.2 mL saline, hydrogel, or hydrogel + MFG-E8 (that underwent 10 s of irradiation) was injected into the bone tunnels of different experimental groups through a syringe. A needle was inserted in the bone tunnel to allow the tendon graft to pass through. The proximal end of the tendon graft was fixed using a micro endo-button at the exit site of the femoral tunnel. The tendon graft was then subjected to a pre-tensioning force of 1 N using a weight hung over a pulley, and the distal end was simultaneously secured to the cortical bone and surrounding periosteum at the tibial exit tunnel site. The wounds were closed using routine procedures (Fig. 2). Free cage movement was allowed for all animals after surgery. Animals from different groups were sacrificed by lethal anaesthetic overdose at specific postoperative time points. The harvested specimens were trimmed to a specific size and shape according to different experimental requirements.

### 2.10. Micro-CT analysis

The femur-tendon graft-tibia (FTGT) complexes (n = 6 per group) were harvested at 4, 8, and 12 weeks post-surgery. Six specimens in each group were scanned perpendicular to the long axis of the bone tunnels using the SkyScan 1176 micro-CT system (SkyScan, Bruker, GER) after fixation in 4% paraformaldehyde for 24 h. The resolution ratio was 35 mm, the voltage was 55 kV, the current was 378 mA, and the voxel size was 18 μm. A region of interest (ROI) 1.6 mm in diameter was selected at the centre of the bone tunnel below the tibial epiphysis for 3D reconstruction. The bone mineral density (BMD), trabecula bone volume fraction (BV/TV), bone surface/bone volume (BS/BV), trabecular thickness (Tb. Th), trabecular number (Tb. N), and trabecular separation (Tb. Sp) of the selected ROIs were analysed. Immediately after the micro-CT scanning, the samples were decalcified with 15% EDTA for histological examination.

### 2.11. Histological analysis

After decalcification, samples were embedded in paraffin wax and sectioned using a microtome at 5-μm-thickness parallel to the longitudinal axis of the tibia bone tunnel. Haematoxylin and eosin (H&E) staining was performed to identify the interface zone between the tendon graft and the bone. Histological assessment focused on the integrity, degree of tendon-bone integration, new bone formation, and Sharpey-like fibres. The average of the maximum width between the tendon and bone at a depth of 1 mm (range, 1 mm) from the tibial epiphyseal plate was calculated as the mean interface width of each group.

### 2.12. Biomechanical test

At 4, 8, and 12 weeks post-surgery, the FTGT complexes were harvested (six in each group). Suture materials, micro endo-button and soft tissues, except for the tendon graft, were freed and carefully dissected. Biomechanical testing was performed using an Instron 5940 universal

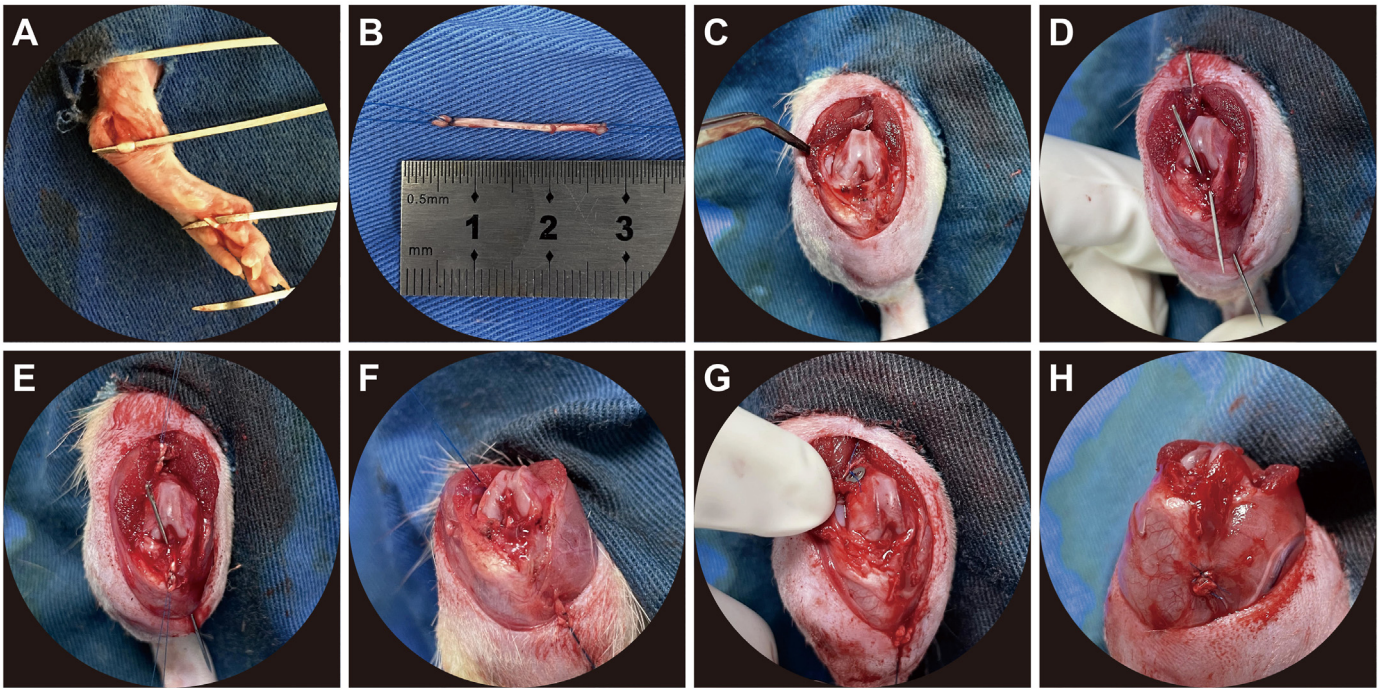


**Figure 2.** ACLR procedures (A) FDL was harvested and used as the tendon graft (B) Ends of the tendon graft were reinforced, the length was measured and recorded (C) The knee joint was exposed through lateral patellar dislocation, and the native ACL was transacted (D) 1.2 mm-diameter bone tunnel was drilled. A needle was inserted into the bone tunnel (E) Needles were used to help the tendon graft pass through (F) The tendon graft was successfully passed from the femoral bone tunnel to the tibial bone tunnel (G) The proximal end of the tendon graft was fixed with a micro endo-button at the femoral tunnel exit site (H) The distal end was secured to the cortical bone and surrounding periosteum at the tibial exit tunnel site. ACLR, anterior cruciate ligament reconstruction; FDL, flexor digitorum longus.

testing system (Instron, Boston, MA, USA). The FTGT complex was fixed and an axial load was applied in a direction aligned with the long axis of the graft. Each sample was preconditioned with 5 cycles of longitudinal loads of 1 N, and then stretched at a speed of 0.2 mm/s until gross failure of the reconstructed ACL occurred. The maximal failure load and stiffness were obtained from the load–displacement curves.

### 2.13. Immunohistochemical (IHC) and TUNEL staining

FTGT complexes (n = 3 per group) were harvested at days 5 and 10 post-surgery to assess early changes in macrophage polarisation and cell apoptosis at the interface between the tendon graft and bone tunnel. After being fixed and decalcified by EDTA decalcifying solution, samples were embedded in paraffin wax and sectioned at 5-μm-thickness perpendicular to the longitudinal axis of the tendon graft.

Immunohistochemistry (IHC) was performed using the standard method. Sections were incubated with the primary antibodies iNOS or CD206 (1:200; Abcam, Cambridge, UK) in a humid chamber at 4 °C overnight, followed by the application of a horseradish peroxidase (HRP) -labelled secondary antibody. Finally, diaminobenzidine (DAB) was used to detect the antibody–antigen complex of interest. After IHC staining, the positive area ratios of iNOS and CD206 in the captured images were measured using Image-Pro Plus.

TUNEL staining of the sections was performed to detect apoptotic cells using the One Step TUNEL Apoptosis Assay Kit (Beyotime, Shanghai, China), according to the manufacturer's instructions. Each slice was incubated with 50 μL TUNEL detection solution at 37 °C for 60 min in the dark. One section was selected in each FTGT complex, and the number of TUNEL-positive apoptotic cells around the tendon-bone interface was manually counted using a fluorescence microscope.

### 2.14. Western blot analysis

Protein extraction and western blotting of cultured cells or interface tissues were performed during the early stage post-surgery in accordance with published processes. Briefly, after different treatments, proteins were separated using 10% SDS-PAGE and transferred to PVDF membranes. The membranes were blocked with 5% nonfat milk for 2 h and washed with TBST. The following primary antibodies were used in the experiments: iNOS, CD206, IL-1β, IL-10, and β-actin (1:1000 dilution; Abcam, Cambridge, UK). Protein bands were detected using the Quantity One software (Bio-Rad, Hercules, CA, USA). β-actin was used as an internal control.

### 2.15. Statistical analysis

All statistical analyses were performed using GraphPad Prism 8 (GraphPad Software, SanDiego, CA, USA). Data are presented as mean ± standard deviation and were analysed using Student's t-test when normally distributed. Nonparametric data were analysed using the Mann–Whitney U test. Analysis of variance was performed for multiple group comparisons. Statistical significance was set at $P < 0.05$.

## 3. Results

### 3.1. Identification of BMDMs

After 6 days of M-CSF induction, FCM analysis showed that the positivity rate of F4/80 and CD11b in primary BMDMs was 92.2%. Similarly, double IF staining showed high expression levels of F4/80 (red) and CD11b (green). These results indicated the high purity of the obtained BMDMs (Figs. S1A and S1B).

### 3.2. The effect of MFG-E8 on macrophage polarisation

As shown in Fig. 3A, after stimulation with IFN-γ + LPS, IL-4, or MFG-E8 for 24 h, BMDMs showed different morphologies under a microscope. The cells in the control group were spindle-shaped, triangular, or

polygonal with smooth surfaces. Cells in the IFN-γ + LPS group were mainly elongated and polygonal with multiple, longer filopodia. Cells in the IL-4 group were fusiform, triangular, or polygonal with pseudopodia of different lengths. Cell morphology in the MFG-E8 group more closely resembled that in the IL-4 group. FCM analysis revealed that IFN-γ + LPS and IL-4 could significantly upregulate the positive rate of CD86 and CD206, respectively, whereas MFG-E8 had no significant effect on macrophage polarisation (Fig. 3B). In accordance with changes in macrophage polarisation, the concentrations of pro-inflammatory cytokines (IL-1β and TNF-α) and anti-inflammatory cytokines (IL-10 and Arg-1) also changed. The mRNA levels of pro-inflammatory cytokines increased significantly after IFN-γ + LPS stimulation, whereas those of anti-inflammatory cytokines increased remarkably after IL-4 stimulation. In addition, MFG-E8 alone did not promote the release of inflammation-related cytokines (Fig. 3C).

Interestingly, IF staining of iNOS and CD206 demonstrated that supplementation with 20 ng/mL MFG-E8 could partially reverse the expression of iNOS and the morphological changes in M1 macrophages, but could not increase CD206 expression in M2 macrophages, as compared to the BMDMs stimulated with IFN-γ + LPS or IL-4 alone. This indicates a potential direct anti-inflammatory effect of MFG-E8 in cellular inflammation induced by IFN-γ + LPS (Fig. 3D).

### 3.3. MFG-E8 promotes macrophage M2 polarisation via enhanced efferocytosis

First, PMNs were obtained by Percoll density gradient centrifugation. Using modified Giemsa staining, a typical PMNs appearance was observed (Fig. S2A). FCM analysis showed that the proportion of double-positive Ly6G and CD11b cells was 86.1%, while the expression of F4/80 was negative (Fig. S2B), and the percentage of apoptotic cells in the starvation medium for 48 h was over 40% (Fig. S2C).

As visualised using fluorescence microscopy, a stepwise increase in the concentration of MFG-E8 was accompanied by an increase in the number of BMDMs (red) containing apoptotic PMNs (green). Interestingly, the efferocytosis index was suppressed as the concentration of MFG-E8 further increased (Fig. 4A and B). These results indicate that there is a threshold concentration of MFG-E8 for macrophage efferocytosis, and 500 ng/mL was the most effective in the current study. Thus, 500 ng/mL of MFG-E8 was used in subsequent experiments. Western blot analysis further revealed that when cells were treated with 500 ng/mL MFG-E8, the expression of CD206 in the co-culture system was significantly higher than that in the control group, while the expression of iNOS was significantly decreased (Fig. 4C). Therefore, these results demonstrate that MFG-E8 promotes macrophage efferocytosis and induces macrophage M2 polarisation.

### 3.4. Characterisation of the MFG-E8 and hydrogel mixture

The MFG-E8 and GelMA mixture was fluid-like before UV light irradiation at 37 °C and could transform into a slightly viscous liquid gel when irradiated with 405 nm UV light for 10 s at 37 °C, while the injectability was maintained (Fig. S3A). The properties of the mixtures were evaluated further. First, the release of MFG-E8 from GelMA was examined. MFG-E8 exhibited a release behaviour with initial bursts of 79.6% from days 0–11. A total of 88.6% of MFG-E8 was released from the mixture after 20 days (Fig. S3B). Second, the in vitro degradation behaviour was investigated. As shown in Figs. S3C and a degradation curve similar to the release performance was obtained, and 84.7% weight loss of the mixture was achieved after 20 days, indicating that the mixture had good degradability. Collectively, these data indicated that the mixture could be injected through a syringe and then adhere to the bone tunnel, and most of the MFG-E8 could be released in approximately 11 days with a consecutive sustained-release phase up to 20 days, which overlaps with the degradation period of the mixture.

### 3.5. MFG-E8 promotes tendon-bone healing in an ACLR model

To investigate whether MFG-E8 could promote tendon-bone healing, a rat ACLR model was successfully established for in vivo experiments. Micro-CT scanning protocols (Fig. 5A) and the 3D reconstruction images demonstrated that significantly increased peri-tunnel bone tissues below the tibial epiphyseal plate were found in the MFG-E8 group at specific time points post-surgery (Fig. 5B). Microarchitectural parameter analysis showed that the peri-tunnel bone tissues of the MFG-E8 group had significantly higher BMD, BV/TV, Tb. Th, and Tb. N than those in the control and hydrogel groups at 4, 8, and 12 weeks post-surgery. Tb. Sp levels were significantly higher in the MFG-E8 group than that in the other two groups at 8 and 12 weeks, but not at 4 weeks. In addition, no significant difference was detected in BS/BV among the three groups post-surgery (Fig. 5C). These results indicate that a significantly greater area of new bone was formed at the tendon-bone interface in the MFG-E8 group, compared to that in the other two groups.

The fibrous interface width between the tendon graft and bone tunnel has been recognised as a vital indicator for evaluating the quality of tendon-bone healing, and a thinner interface suggests better integration [19,20]. As shown in Fig. 5D, a distinct tendon-bone interface and disordered fibrovascular tissues were observed in all three groups at 4 weeks post-surgery, and a narrower interface width was observed in the MFG-E8 group than in the other two groups. At 8 weeks after surgery, reduction of the interface width was found in all groups; however, Sharpey-like fibres (white arrows) connecting the newly formed bone were first observed in the MFG-E8 group, but not in the other two groups. In addition, more osseous ingrowth into the interface, better tendon remodelling, and barely any visible gaps were observed in the MFG-E8 group at 12 weeks post-surgery.

We next performed biomechanical tests on the FTGT complexes (Fig. 5E). At specific time points, the maximum failure load and stiffness in the MFG-E8 group were always significantly better than those in the control and hydrogel groups (Fig. 5F), suggesting that MFG-E8 treatment resulted in better healing at the tendon-bone interface.

### 3.6. MFG-E8 promotes macrophage efferocytosis and M2 polarisation at early stage in vivo

IHC results showed that, as time progressed, the positive areas of iNOS and CD206 changed at the tendon-bone interface in both groups. Moreover, compared to the control group, the MFG-E8 group showed a significant reduction in the iNOS-positive area and a significant increase in the CD206-positive area at days 5 and 10 post-surgery, respectively (Fig. 6A).

As shown in Fig. 6B, TUNEL staining revealed apoptotic cells (green) at the tendon-bone interface in the different groups, with fewer green cells indicating fewer apoptotic cells. When compared with the control group, the MFG-E8 group was found to have a reduced number of apoptotic cells at both days 5 and 10 post-surgery, indicating that apoptotic cells are efficiently recognised and cleared by phagocytes.

Western blot analysis further confirmed that the expression levels of iNOS and IL-1β decreased in the MFG-E8 group after surgery, whereas CD206 and IL-10 expression levels were significantly higher, especially on day 10 post-surgery (Fig. 6C).

Collectively, these observations confirmed that treatment with MFG-E8 promoted macrophage efferocytosis and M2 polarisation while alleviating the inflammatory response of the tendon-bone interface during the early stage after surgery (Fig. 6D).

## 4. Discussion

To the best of our knowledge, this is the first study to investigate the association between MFG-E8, macrophage efferocytosis, macrophage polarisation, and tendon-bone healing in an ACLR model. Our current study has four major findings. First, macrophage efferocytosis was

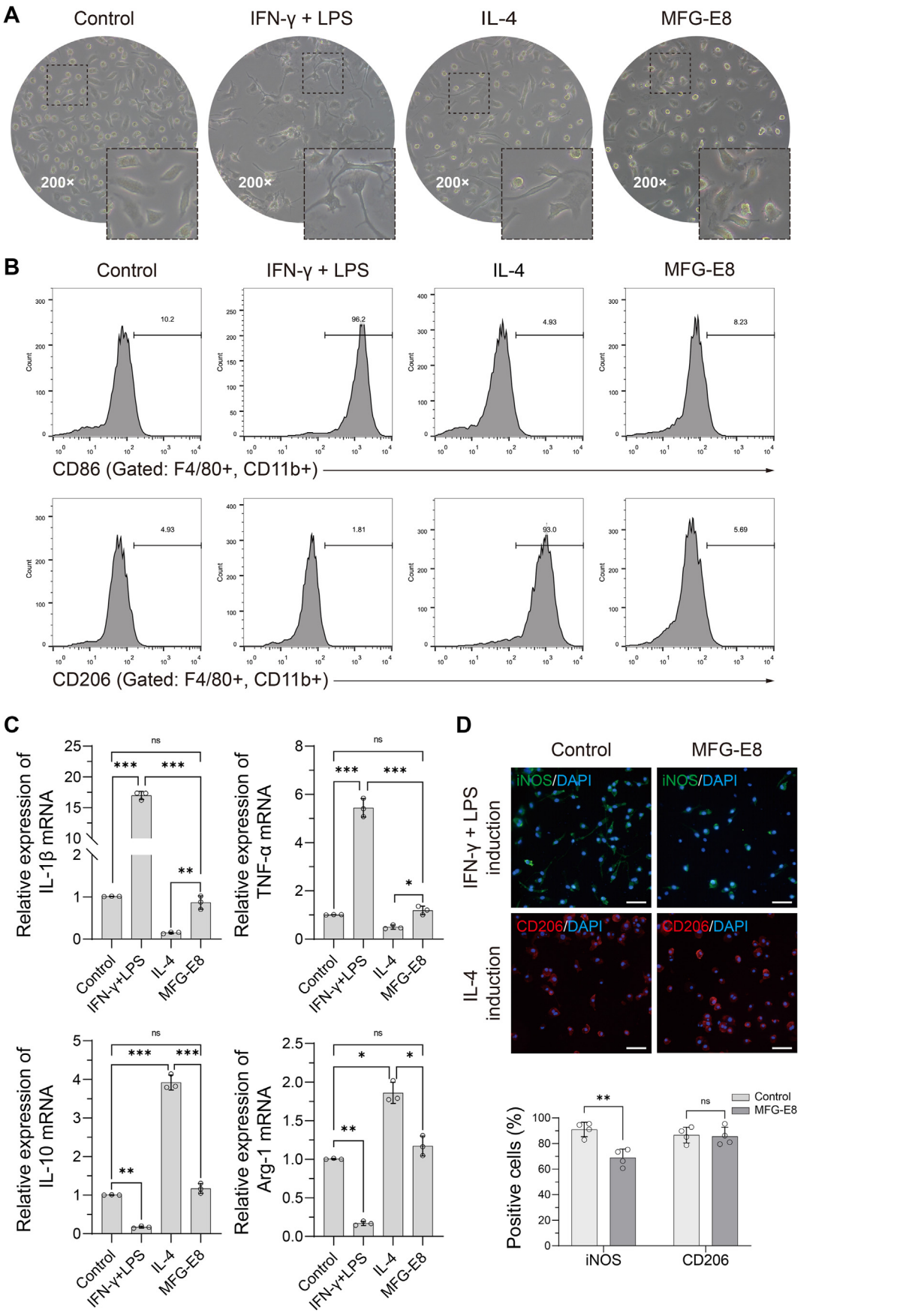


*(caption on next page)*

**Figure 3.** Effects of MFG-E8 on macrophage polarisation (A) The morphology of BMDMs were observed using a microscope after IFN-γ+ LPS, IL-4 or MFG-E8 stimulation for 24 h (B) The activation-related surface markers of BMDMs were analysed by FCM. When compared with the control group (untreated), a significant shift of CD86+ and CD206+ macrophages were observed in the IFN-γ+ LPS and IL-4 groups, respectively, at 24 h after stimulation, but not in the MFG-E8 group. N = 3 per group (C) Relative mRNA expression levels of inflammatory cytokines were detected in BMDMs after different stimulations for 24 h N = 3 per group. *$P$ < 0.05, **$P$ < 0.01, ***$P$ < 0.001 (D) IF staining of iNOS or CD206 demonstrated that MFG-E8 could partially reverse the expression of iNOS in M1 macrophages, but could not increase the CD206 expression in M2 macrophages. Scale bar = 100 μm N = 4 per group. **$P$ < 0.01. BMDM, bone marrow derived macrophage; IFN-γ, interferon γ; LPS, lipopolysaccharide; IL-4, interleukin-4; MFG-E8, milk fat globulin protein E8; FCM, flow cytometry.

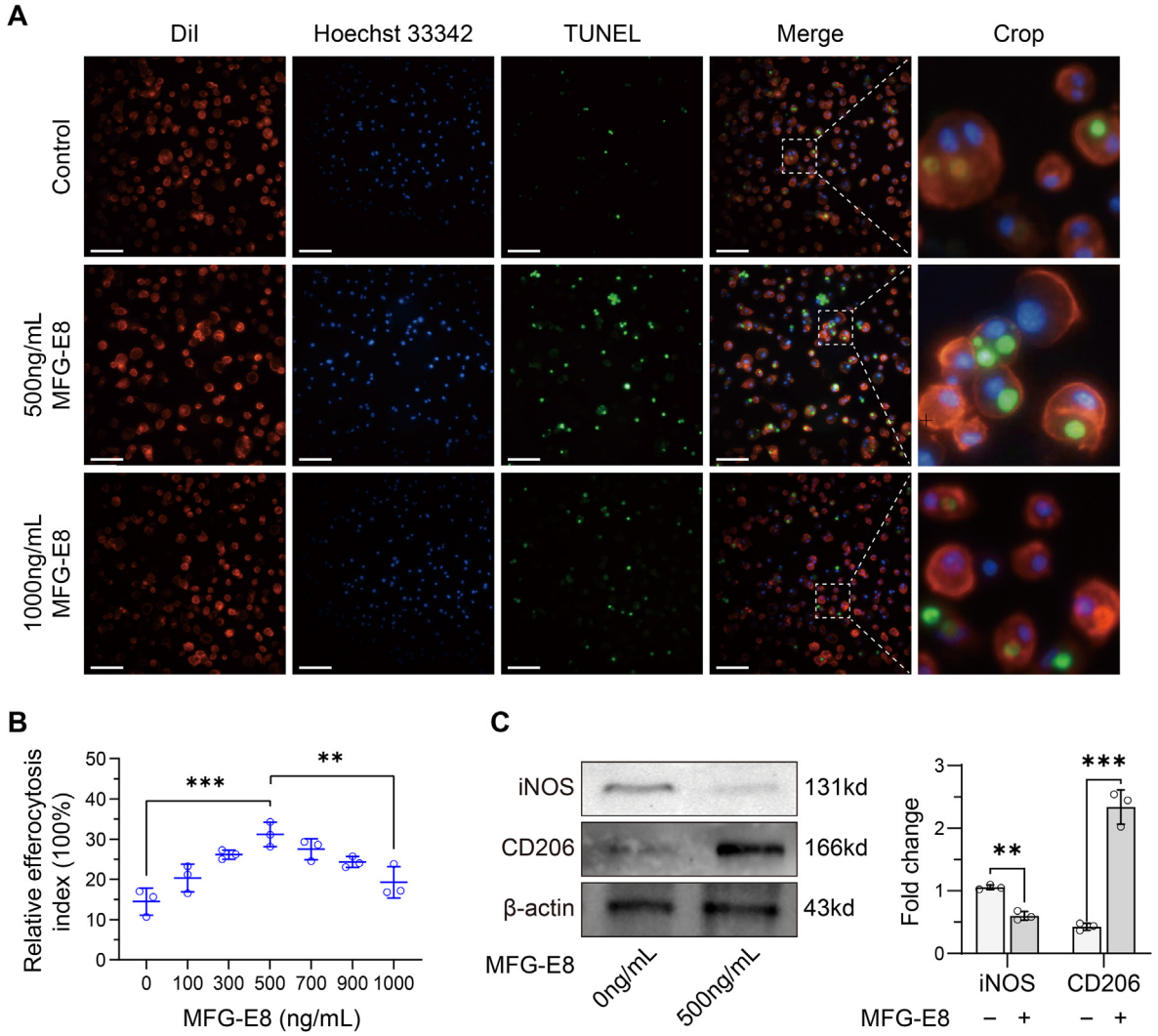


**Figure 4.** Efferocytosis assay (A) Different doses of MFG-E8 were co-cultured for 2 h, and the clearance of apoptotic PMNs by BMDMs was viewed by fluorescent staining. Apoptotic PMNs appeared in green and BMDMs appeared in red. Scale bar = 100 μm (B) The relative efferocytosis index were calculated from fluorescent staining images. Increasing concentrations of MFG-E8 generated a parabolic-shaped response curve for the efficiency of efferocytosis. N = 3 per group. **$P$ < 0.01, ***$P$ < 0.001 (C) The expression levels of iNOS and CD206 were evaluated by western blot analysis. N = 3 per group. **$P$ < 0.01, ***$P$ < 0.001. MFG-E8, milk fat globulin protein E8; BMDM, bone marrow derived macrophage; PMN, polymorphonuclear neutrophil.

enhanced by the addition of an appropriate dose of MFG-E8 when co-cultured with apoptotic cells. Second, efferocytosis enhanced by MFG-E8 could also promote macrophage M2 polarisation, which was beneficial for the secretion of anti-inflammatory cytokines. Third, more new bone formation, more mature interface tissues, and better mechanical properties at the tendon-bone interface were observed in the MFG-E8 treatment group. Finally, the local application of MFG-E8 at the tendon-bone interface promoted the clearance of apoptotic cells and macrophage M2 polarisation during the early stage after surgery. Therefore, MFG-E8 plays a positive role in ACLR and is expected to improve clinical outcomes.

Tissue injury leads to instant activation of the local inflammatory response, which is characterised by massive infiltration of neutrophils at the initial site. Proper termination of this inflammatory cascade is important for tissue repair and the restoration of normal tissue function. In healthy individuals, the clearance of apoptotic cells is quiet and is not associated with an inflammatory response; however, apoptotic cells in inflammatory tissues contain a large number of cytotoxic compounds. If not cleared in time, the prolonged presence of these cells aggravates inflammation, which could result in chronic inflammation and excessive scar formation. Interesting studies of foetal wounds suggest that without the recruitment of inflammatory cells, wounds heal through tissue regeneration instead of scar formation [21], whereas during late pregnancy, foetal wounds heal by fibrotic scar formation [22], suggesting that

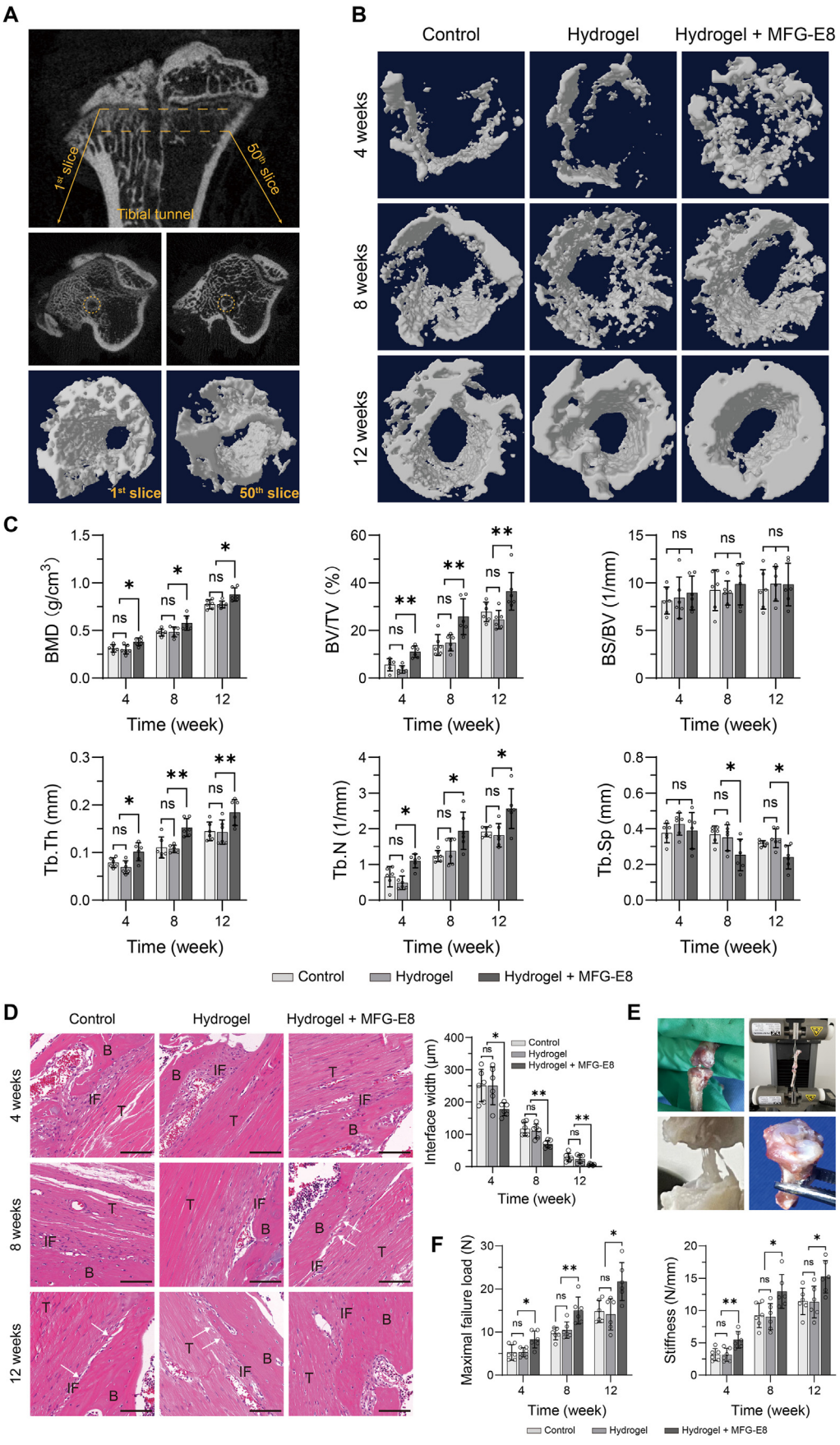


**Figure 5.** Effects of MFG-E8 on tendon-bone healing (A) Micro-CT scanning protocols. A total of 50 slices below the tibial epiphysis were selected for creating 3D images of the ROIs (B) 3D reconstruction of the peri-tunnel bone tissue from different treatment groups at specific time points after surgery (C) Micro-architectural parameters of the peri-tunnel bone tissue was measured by micro-CT. n = 6 per group. $^{*}P < 0.05$, $^{**}P < 0.01$ (D) H&E staining was used to evaluate the interface tissues between bone tunnel and tendon graft, with quantification of the width of the tendon-bone interface. White arrows indicate Sharpey-like fibres. Scale bar = 100 μm N = 6 per group. $^{*}P < 0.05$, $^{**}P < 0.01$ (E) Biomechanical test protocols using the Instron universal testing systems (F) Biomechanical test results, maximal failure load and stiffness of the specimens were obtained from the load–displacement curve. N = 6 per group. $^{*}P < 0.05$, $^{**}P < 0.01$. MFG-E8, milk fat globulin protein E8; ROI, region of interest; H&E, hematoxylin and eosin; BMD, bone mineral density; BV/TV, trabecula bone volume fraction; BS/BV, bone surface/bone volume; Tb. Th, trabecular thickness; Tb. N, trabecular number; Tb. Sp, trabecular separation; B, bone; T, tendon graft; IF, interface.

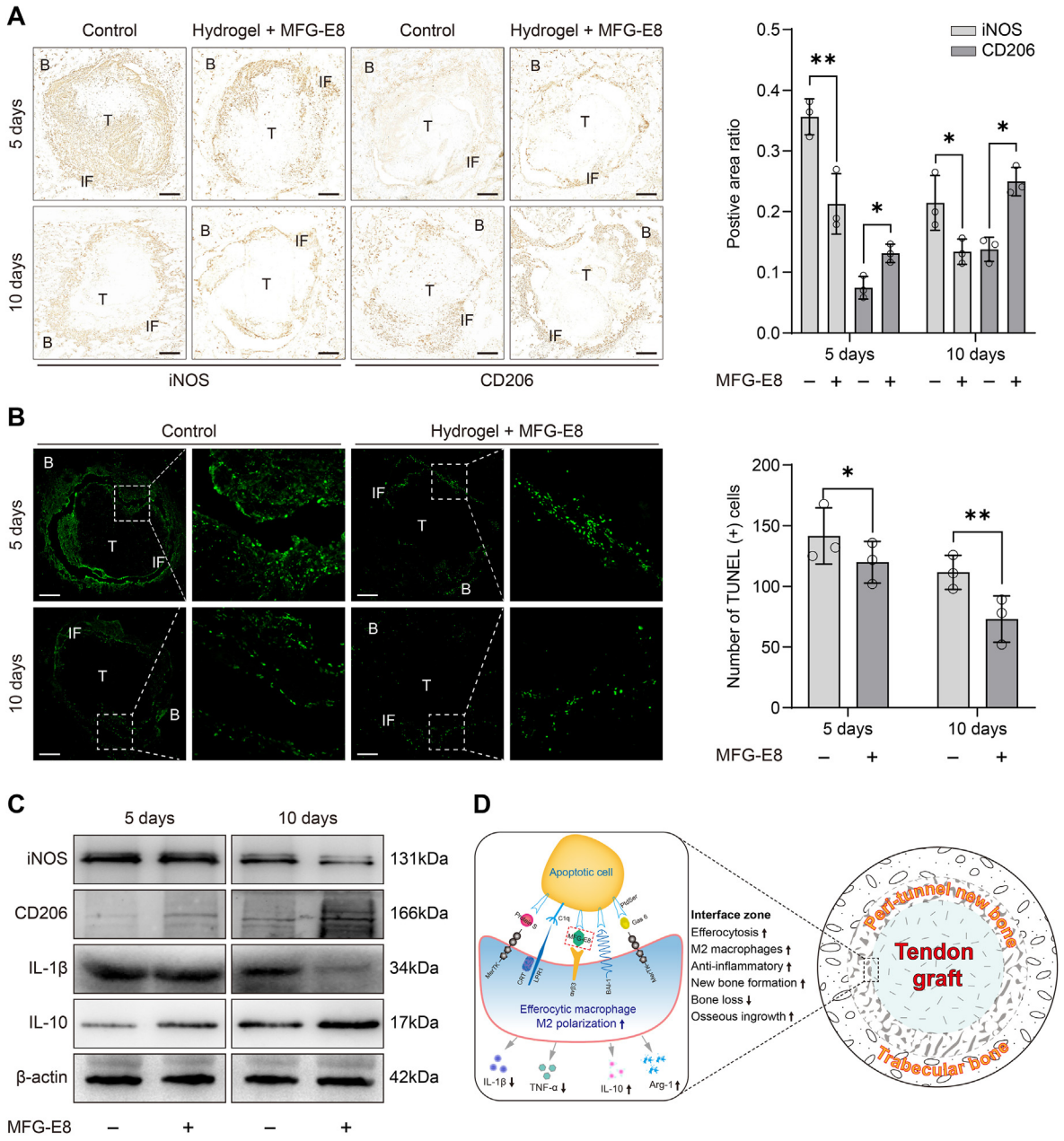


**Figure 6.** Effects of MFG-E8 on macrophage efferocytosis and M2 polarisation in vivo (A) IHC staining of iNOS and CD206 at the tendon-bone interface of the control group and the MFG-E8 group at 5 and 10 days after surgery. Scale bar = 200 μm N = 3 per group. $^{*}P < 0.05$, $^{**}P < 0.01$ (B) Apoptotic cells (in green) at the tendon-bone interface were detected by TUNEL staining. Bar graph represents the quantification of the TUNEL-positive apoptotic cells around the tendon-bone interface. Scale bar = 200 μm N = 3 per group. $^{*}P < 0.05$, $^{**}P < 0.01$ (C) The expression levels of iNOS, CD206, IL-1β, and IL-10 in tendon-bone interface tissues at 5 and 10 days after surgery were evaluated by western blot analysis. N = 3 per group. $^{*}P < 0.05$, $^{**}P < 0.01$, $^{***}P < 0.001$ (D) Schematic diagram of the mechanisms behind the promotive effects of the macrophage efferocytosis and M2 polarisation in the tendon-bone healing. IHC, immunohistochemical; MFG-E8, milk fat globulin protein E8; B, bone; T, tendon graft; IF, interface.

acute inflammation may not be necessary for adequate tissue repair [23].

Efferocytosis is the process by which dying cells are engulfed and digested by phagocytes, especially macrophages, which can migrate along a chemokine gradient and carry out most efferocytic cell removal. The term refers specifically to phagocytosis of apoptotic cells rather than other phagocytic processes [24]. Without proper efferocytosis, apoptotic cells can undergo secondary necrosis following the release of potentially harmful cellular products that can induce an excessive inflammatory response [25]. Previous studies have shown that efferocytosis can create an anti-inflammatory environment [8,26]. The complete efferocytosis process includes the following: first, efferocytes sense "find-me" signals released by apoptotic cells, while normal cells express "don't-eat-me" signals; second, "eat-me" signals are recognised by efferocytic receptors and apoptotic cells are engulfed; and lastly, apoptotic bodies are processed into efferosomes, and cytokines are released by efferocytes in the post-engulfment stage.

MFG-E8 is a secreted multifunctional glycoprotein that acts as a bridge for macrophages to recognise "eat-me" signals expressed on the surface of apoptotic cells, which could facilitate the clearance of apoptotic cells and pro-inflammatory cytokines and eventually prevent secondary injury. Furthermore, MFG-E8 could shift the microglial phenotype toward M2 polarisation, alleviate the symptoms of Alzheimer's disease by modulating the M1/M2 polarisation [27], and play a key role in tissue healing through induction of the M2 phenotype [28]. In

the present study, we found that MFG-E8 promotes the engulfment of apoptotic cells by macrophages. Moreover, not only could macrophage efferocytosis be enhanced by MFG-E8, but efferocytosis could also in turn promote M2 polarisation, which seems to create a virtuous cycle of an anti-inflammatory microenvironment. However, the effect of MFG-E8 on efferocytosis was dose-dependent and generated a parabolic-shaped response curve, which means that only the appropriate concentration will enhance the maximum activity. This might be because sufficient MFG-E8 saturated the binding sites on apoptotic cells and macrophages at high concentrations, preventing further binding of these cells. This phenomenon is similar to the process of growth hormone action. Additionally, Morioka et al. confirmed that efferocytic phagocytes can influence macrophages in the tissue neighbourhood toward anti-inflammatory polarisation via SLC16A1 mediated lactate release [29]. Das et al. suggested that efferocytosis serves as a cue for M0 switching to an anti-inflammatory M2 phenotype [30]. Therefore, it is conceivable that the effects of MFG-E8 are dependent on its effects on efferocytosis and subsequent M2 polarisation.

Interestingly, we found that 20 ng/mL MFG-E8 could partially reverse the expression of iNOS in M1 macrophages, but could not increase CD206 expression in M2 macrophages, indicating a potential direct anti-inflammatory effect of MFG-E8 on pro-inflammatory cells. One possible explanation for this phenomena is that MFG-E8 could directly modulating TLR4 signaling through its binding to αvβ3 integrin [31], which attenuated inflammation but not due to phagocytic engulfment.

Rodeo et al. demonstrated that without any interventions, neutrophils and M1 macrophages were first identified at the tendon-bone interface, while M2 macrophages were not observed until 11 days post-surgery [6], which was similar to our findings. In our work, 79.6% MFG-E8 could be continuously released for approximately 11 days from the injectable hydrogel, which overlaps with the inflammatory period of macrophage infiltrating the tendon-bone interface. Using MFG-E8 in vivo could promote the early appearance of CD206 (M2 marker) and reduce the expression of iNOS (M1 marker) at the interface region. Furthermore, a previous study confirmed that using biological interventions to induce M2 macrophages to accumulate at the tendon-bone interface at an early stage postoperatively was beneficial to tendon-bone healing [32]. Collectively, these findings indicate that MFG-E8 plays a vital role in regulating the inflammatory microenvironment by modulating macrophage efferocytosis and M2 polarisation in tendon-bone healing.

Since the native enthesis is a gradient region consisting of tendon, non-mineralised fibrocartilage, mineralised fibrocartilage, and bone [33], scientists have tried various methods to achieve the ideal highly specialised transition interface; however, the therapeutic effects are still controversial. Current researchers believe that the biomechanical properties of the interface are associated with osseous ingrowth and osteointegration, whereas Sharpey-like fibres denote early signs of osteointegration [20,34,35]. In addition, a diminished width and better fibre arrangement at the tendon-bone interface were observed in the enhanced M2 polarisation group [36]. Our micro-CT findings revealed that animals in all groups had increased microarchitectural parameters from 4 to 12 weeks, but the MFG-E8 group demonstrated more peri-tunnel bone formation and bony ingrowth. This may be associated with the novel ability of MFG-E8 to inhibit inflammatory bone loss and maintain bone homeostasis by regulating bone marrow-derived osteoclast precursors [11,37,38]. Histological analysis revealed that the interface was filled with disordered fibrovascular tissue at 4 weeks and narrowed at 8–12 weeks after surgery in all groups. However, at 8 weeks, the MFG-E8 group showed more distinct Sharpey-like fibres, better fibre arrangement, and a significantly diminished width of the interface region. All these events ultimately led to significantly better outcomes for maximal failure load and stiffness.

However, our study had some limitations. First, given a greater self-healing potential of rodent than that of human and rodent are not perfect models to study human disease, it is important to investigate the effectiveness of MFG-E8 in large mammals. Second, owing to the convenience of the surgical procedures, we employed rats as animal models, and further experiments using genetically modified MFG-E8$^{-/-}$ or macrophage-depleted mice are required to verify these findings. Third, TUNEL staining is not specific to PMNs, and to draw more robust evidence, further double fluorescence of apoptotic PMNs (TUNEL and PMN-specific immunofluorescence staining) is required. However, the result of TUNEL staining here will, at the very least, provide an indication of more apoptotic cell clearance. Lastly, the results of in vitro experiments did not adequately represent the real situation in vivo, and MFG-E8 at 500 ng/mL must be considered preliminary. Further in vivo studies are required to determine the optimal dosage.

## 5. Conclusions

In the current study, we found that MFG-E8 attenuated the inflammatory response via enhanced macrophage efferocytosis and M2 polarisation, which ultimately resulted in reduced inflammatory bone loss, increased peri-tunnel new bone formation, and improved osteointegration. Thus, MFG-E8 could act as a new therapeutic strategy for enhancing tendon-bone healing in patients undergoing ACLR.

## Author contributions

All authors contributed to the study conception. JL and MLJ are responsible for project planning. RG, YCL and QC conducted the expreriments, ZL, LX and WTZ analyzed the data. RG and YCL wrote the first draft of the manuscript. JL and MLJ revised the manuscript. All authors read and approved the final manuscript.

## Funding

This study was supported by the National Natural Science Foundation of China (Grant No. 82072427).

## Declaration of competing interest

The authors have no conflicts of interest relevant to this article.

## Acknowledgements

The authors thank Elsevier Language Editing Services for scientific English editing.

## Appendix A. Supplementary data

Supplementary data to this article can be found online at https://doi.org/10.1016/j.jot.2022.04.002.

## References

[1] Kaeding CC, Léger-St-Jean B, Magnussen RA. Epidemiology and diagnosis of anterior cruciate ligament injuries. Clin Sports Med 2017;36(1):1–8. https://doi.org/10.1016/j.csm.2016.08.001.
[2] Song B, Jiang C, Luo H, Chen Z, Hou J, Zhou Y, et al. Macrophage M1 plays a positive role in aseptic inflammation-related graft loosening after anterior cruciate ligament reconstruction surgery. Inflammation 2017;40(6):1815–24. https://doi.org/10.1007/s10753-017-0616-3.
[3] Camp CL, Lebaschi A, Cong G, Album Z, Carballo C, Deng X, et al. Timing of postoperative mechanical loading affects healing following anterior cruciate ligament reconstruction. J Bone Joint Surg Am 2017;99(16):1382–91. https://doi.org/10.2106/JBJS.17.00133.
[4] Borthwick LA, Wynn TA, Fisher AJ. Cytokine mediated tissue fibrosis. Biochim Biophys Acta 2013;1832(7):1049–60. https://doi.org/10.1016/j.bbadis.2012.09.014.
[5] Derwin KA, Galatz LM, Ratcliffe A, Thomopoulos S. Enthesis repair. J Bone Joint Surg Am 2018;100(16):e101–9. https://doi.org/10.2106/JBJS.18.00200.
[6] Kawamura S, Ying L, Kim H, Dynybil C, Rodeo SA. Macrophages accumulate in the early phase of tendon–bone healing. J Orthop Res 2005;23(6):1425–32. https://doi.org/10.1016/j.orthres.2005.01.014.1100230627.

[7] Mantovani A, Cassatella MA, Costantini C, Jaillon S. Neutrophils in the activation and regulation of innate and adaptive immunity. Nat Rev Immunol 2011;11(8):519–31. https://doi.org/10.1038/nri3024.
[8] Elliott MR, Koster KM, Murphy PS. Efferocytosis signaling in the regulation of macrophage inflammatory responses. J Immunol 2017;198(4):1387–94. https://doi.org/10.4049/jimmunol.1601520.
[9] Aziz M, Matsuda A, Yang WL, Jacob A, Wang P. Milk fat globule-epidermal growth factor-factor 8 attenuates neutrophil infiltration in acute lung injury via modulation of CXCR2. J Immunol 2012;189(1):393–402. https://doi.org/10.4049/jimmunol.1200262.
[10] Gao Y, Tao T, Wu D, Zhuang Z, Lu Y, Wu L, et al. MFG-E8 attenuates inflammation in subarachnoid hemorrhage by driving microglial M2 polarization. Exp Neurol 2021;336:113532. https://doi.org/10.1016/j.expneurol.2020.113532.
[11] Michalski MN, Seydel AL, Siismets EM, Zweifler LE, Koh AJ, Sinder BP, et al. Inflammatory bone loss associated with MFG-E8 deficiency is rescued by teriparatide. Faseb J 2018;32(7):3730–41. https://doi.org/10.1096/fj.201701238R.
[12] Uchiyama A, Yamada K, Ogino S, Yokoyama Y, Takeuchi Y, Udey MC, et al. MFG-E8 regulates angiogenesis in cutaneous wound healing. Am J Pathol 2014;184(7):1981–90. https://doi.org/10.1016/j.ajpath.2014.03.017.
[13] Shi Z, Zhang Y, Wang Q, Jiang D. MFG-E8 regulates inflammation and apoptosis in tendon healing, and promotes tendon repair: a histological and biochemical evaluation. IUBMB Life 2019;71(12):1986–93. https://doi.org/10.1002/iub.2143.
[14] Rios FJ, Touyz RM, Montezano AC. Isolation and differentiation of murine macrophages. Methods Mol Biol 2017;1527:297–309. https://doi.org/10.1007/978-1-4939-6625-7_23.
[15] Dong X, Wu D. Methods for studying neutrophil chemotaxis. Methods Enzymol 2006;406:605–13. https://doi.org/10.1016/S0076-6879(06)06047-2.
[16] Kourtzelis I, Li X, Mitroulis I, Grosser D, Kajikawa T, Wang B, et al. DEL-1 promotes macrophage efferocytosis and clearance of inflammation. Nat Immunol 2019;20(1):40–9. https://doi.org/10.1038/s41590-018-0249-1.
[17] Carbone A, Carballo C, Ma R, Wang H, Deng X, Dahia C, et al. Indian hedgehog signaling and the role of graft tension in tendon-to-bone healing: evaluation in a rat ACL reconstruction model. J Orthop Res 2016;34(4):641–9. https://doi.org/10.1002/jor.23066.
[18] Zong JC, Ma R, Wang H, Cong GT, Lebaschi A, Deng XH, et al. The effect of graft pretensioning on bone tunnel diameter and bone formation after anterior cruciate ligament reconstruction in a rat model. Am J Sports Med 2017;45(6):1349–58. https://doi.org/10.1177/0363546516686967.
[19] Sun Y, Chen W, Hao Y, Gu X, Liu X, Cai J, et al. Stem cell-conditioned medium promotes graft remodeling of midsubstance and intratunnel incorporation after anterior cruciate ligament reconstruction in a rat model. Am J Sports Med 2019;47(10):2327–37. https://doi.org/10.1177/0363546519859324.
[20] Wang J, Xu J, Wang X, Sheng L, Zheng L, Song B, et al. Magnesium-pretreated periosteum for promoting bone-tendon healing after anterior cruciate ligament reconstruction. Biomaterials 2021;268:120576. https://doi.org/10.1016/j.biomaterials.2020.120576.
[21] Hopkinson-Woolley J, Hughes D, Gordon S, Martin P. Macrophage recruitment during limb development and wound healing in the embryonic and foetal mouse. J Cell Sci 1994;107(Pt 5):1159–67. https://doi.org/10.1242/jcs.107.5.1159.
[22] Ashcroft GS, Yang X, Glick AB, Weinstein M, Letterio JJ, Mizel DE, et al. Mice lacking Smad3 show accelerated wound healing and an impaired local inflammatory response. Nat Cell Biol 1999;1(5):260–6. https://doi.org/10.1038/12971.
[23] Larson BJ, Longaker MT, Lorenz HP. Scarless fetal wound healing: a basic science review. Plast Reconstr Surg 2010;126(4):1172–80. https://doi.org/10.1097/PRS.0b013e3181eae781.
[24] Kumar S, Birge RB. Efferocytosis. Curr Biol 2016;26(13):R558–9. https://doi.org/10.1016/j.cub.2016.01.059.
[25] Gheibi Hayat SM, Bianconi V, Pirro M, Sahebkar A. Efferocytosis: molecular mechanisms and pathophysiological perspectives. Immunol Cell Biol 2019;97(2):124–33. https://doi.org/10.1111/imcb.12206.
[26] Jun J, Kim K, Lau LF. The matricellular protein CCN1 mediates neutrophil efferocytosis in cutaneous wound healing. Nat Commun 2015;6(1):7386. https://doi.org/10.1038/ncomms8386.
[27] Xu X, Cai X, Zhu Y, He W, Wu Q, Shi X, et al. MFG-E8 inhibits Aβ-induced microglial production of cathelicidin-related antimicrobial peptide: a suitable target against Alzheimer's disease. Cell Immunol 2018;331:59–66. https://doi.org/10.1016/j.cellimm.2018.05.008.
[28] Laplante P, Brillant-Marquis F, Brissette M, Joannette-Pilon B, Cayrol R, Kokta V, et al. MFG-E8 reprogramming of macrophages promotes wound healing by increased bFGF production and fibroblast functions. J Invest Dermatol 2017;137(9):2005–13. https://doi.org/10.1016/j.jid.2017.04.030.
[29] Morioka S, Perry J, Raymond MH, Medina CB, Zhu Y, Zhao L, et al. Efferocytosis induces a novel SLC program to promote glucose uptake and lactate release. Nature 2018;563(7733):714–8. https://doi.org/10.1038/s41586-018-0735-5.
[30] Das A, Ghatak S, Sinha M, Chaffee S, Ahmed NS, Parinandi NL, et al. Correction of MFG-E8 resolves inflammation and promotes cutaneous wound healing in diabetes. J Immunol 2016;196(12):5089–100. https://doi.org/10.4049/jimmunol.1502270.
[31] Aziz MM, Ishihara S, Mishima Y, Oshima N, Moriyama I, Yuki T, et al. MFG-E8 attenuates intestinal inflammation in murine experimental colitis by modulating osteopontin-dependent alphavbeta3 integrin signaling. J Immunol 2009;182(11):7222–32. https://doi.org/10.4049/jimmunol.0803711.
[32] Lu J, Chamberlain CS, Ji ML, Saether EE, Leiferman EM, Li WJ, et al. Tendon-to-Bone healing in a rat extra-articular bone tunnel model: a comparison of fresh autologous bone marrow and bone marrow-derived mesenchymal stem cells. Am J Sports Med 2019;47(11):2729–36. https://doi.org/10.1177/0363546519862284.
[33] Voleti PB, Buckley MR, Soslowsky LJ. Tendon healing: repair and regeneration. Annu Rev Biomed Eng 2012;14(1):47–71. https://doi.org/10.1146/annurev-bioeng-071811-150122.
[34] Anderson K, Seneviratne AM, Izawa K, Atkinson BL, Potter HG, Rodeo SA. Augmentation of tendon healing in an intraarticular bone tunnel with use of a bone growth factor. Am J Sports Med 2001;29(6):689–98. https://doi.org/10.1177/03635465010290060301.
[35] Mihelic R, Pecina M, Jelic M, Zoricic S, Kusec V, Simic P, et al. Bone morphogenetic protein–7 (osteogenic protein–1) promotes tendon graft integration in anterior cruciate ligament reconstruction in sheep. Am J Sports Med 2017;32(7):1619–25. https://doi.org/10.1177/0363546504263703.
[36] Dagher E, Hays PL, Kawamura S, Godin J, Deng XH, Rodeo SA. Immobilization modulates macrophage accumulation in tendon-bone healing. Clin Orthop Relat Res 2009;467(1):281–7. https://doi.org/10.1007/s11999-008-0512-0.
[37] Abe T, Shin J, Hosur K, Udey MC, Chavakis T, Hajishengallis G. Regulation of osteoclast homeostasis and inflammatory bone loss by MFG-E8. J Immunol 2014;193(3):1383–91. https://doi.org/10.4049/jimmunol.1400970.
[38] Hajishengallis G. MFG-E8, a novel homeostatic regulator of osteoclastogenesis. Inflamm Cell Signal 2014;1(5):e285. https://doi.org/10.14800/ics.285.